X-ray diffraction and inelastic neutron scattering study of 1:1 tetramethylpyrazine chloranilic acid complex: Temperature, isotope, and pressure effects

ARTICLE *in* THE JOURNAL OF CHEMICAL PHYSICS · DECEMBER 2006

Impact Factor: 2.95 · DOI: 10.1063/1.2358347 · Source: PubMed

8 AUTHORS, INCLUDING:

Lucjan Sobczyk
University of Wroclaw
245 PUBLICATIONS **3,560** CITATIONS
SEE PROFILE

Andrzej Pawlukojć
Joint Institute for Nuclear Research
67 PUBLICATIONS **540** CITATIONS
SEE PROFILE

Tilo Seydel
Institut Laue-Langevin
83 PUBLICATIONS **943** CITATIONS
SEE PROFILE

X-ray diffraction and inelastic neutron scattering study of 1:1 tetramethylpyrazine chloranilic acid complex: temperature, isotope, and pressure effects

M. Prager[a),b)]
Institut für Festkörperforschung, Forschungszentrum Jülich, 52425 Jülich, Germany

A. Pietraszko
Institute of Low Temperature and Structure Research, Polish Academy of Sciences, ulica Okolna, 50-950 Wroclaw, Poland

L. Sobczyk[a)]
Faculty of Chemistry, University of Wroclaw, Joliot-Curie 14, 50-383 Wroclaw, Poland

A. Pawlukojć
Institute of Nuclear Chemistry and Technology, ulica Dorodna 16, 03-195 Warsaw, Poland

E. Grech
Institute of Chemistry and Environmental Protection, Szczecin University of Technology, Piastów Aleja 12, 71-065 Szczecin, Poland

T. Seydel
Institut Laue Langevin, 38042 Grenoble, France

A. Wischnewski and M. Zamponi
Institut für Festkörperforschung, Forschungszentrum Jülich, 52425 Jülich, Germany

(Received 29 June 2006; accepted 6 September 2006; published online 21 November 2006)

The x-ray diffraction studies of the title complex were carried out at room temperature and 14 K for H/D (in hydrogen bridge) isotopomers. At 82 K a phase transition takes place leading to a doubling of unit cells and alternation of the hydrogen bond lengths linking tetramethylpyrazine (TMP) and chloranilic acid molecules. A marked H/D isotope effect on these lengths was found at room temperature. The elongation is much smaller at 14 K. The infrared isotopic ratio for O–H(D)···N bands equals to 1.33. The four tunnel splittings of methyl librational ground states of the protonated complex required by the structure are determined at a temperature $T=4.2$ K up to pressures $P=4.7$ kbars by high resolution neutron spectroscopy. The tunnel mode at 20.6 μeV at ambient pressure shifts smoothly to 12.2 μeV at $P=3.4$ kbars. This is attributed to an increase of the strength of the rotational potential proportional to $r^{-5.6}$. The three other tunnel peaks show no or weak shifts only. The increasing interaction with diminishing intermolecular distances is assumed to be compensated by a charge transfer between the constituents of $\delta e/e \sim 0.02$ kbar^{-1}. The phase transition observed between 3.4 and 4.7 kbars leads to increased symmetry with only two more intense tunneling bands. In the isotopomer with deuterated hydrogen bonds and $P=1$ bar all tunnel intensities become equal in consistency with the low temperature crystal structure. The effect of charge transfer is confirmed by a weakening of rotational potentials for those methyl groups whose tunnel splittings were independent of pressure. Density functional theory calculations for the model TMP·$(HF)_2$ complex and fully ionized molecule TMP^+ point out that the intramolecular rotational potential of methyl groups is weaker in the charged species. They do not allow for the unequivocal conclusions about the role of the intermolecular charge transfer effect on the torsional frequencies. © *2006 American Institute of Physics*. [DOI: 10.1063/1.2358347]

I. INTRODUCTION

As shown in reviews on quantum rotation of molecules[1,2] the tunnel splitting of librational states of groups such as CH_3 or NH_3 can yield important information on intermolecular and intramolecular interactions via their rotational potentials. Tunnel splittings are strictly correlated with the shape of rotational potentials and can be recorded by high resolution inelastic neutron spectroscopy (INS). Rotational potentials can be calculated on the basis of a precise crystal structure and intermolecular interaction potentials. Due to its exponential dependence on the height of the rotational barrier rotational tunneling spectroscopy is one of the most sensitive methods to test atom-atom potentials.[3,4] Classical lattice dynamics allows a similar application but the effects are much smaller. For this reason we use here the

[a)]Authors to whom correspondence should be addressed.
[b)]Electronic mail: m.prager@fz-juelich.de

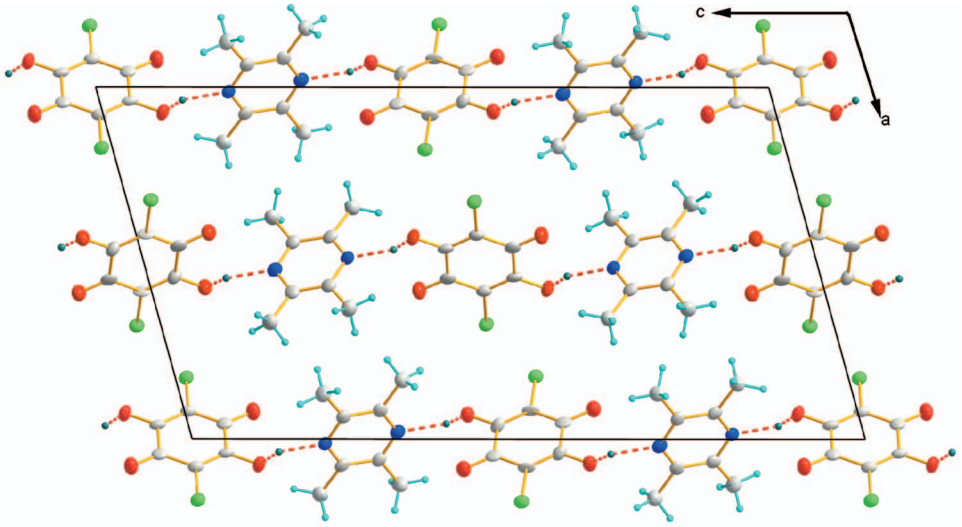

FIG. 1. (Color) Arrangements of TMP and CLA molecules in the crystal of 1:1 TMP·CLA complex at $T=14$ K. Projection along b axis (ellipsoid probability 50%).

tunnel splitting in studies of systems with specific interactions, such as charge transfer and hydrogen bonding.

A sufficient tendency towards such interaction can lead in binary alloys to the formation of stoichiometrically defined complexes with interesting, sometimes new properties. A typical electron donor in such complexes is 1,2,4,5 tetramethyl-benzene, called durene. The pure material was recently successfully studied by neutron spectroscopy.[5,6] While high energy internal modes above ~ 300 cm^{-1} are well described by quantum chemistry models using the GAUSSIAN03 program package,[7] modes in the low frequency regime which are ascribed to rotation and deformation of CH_3 groups substantially depend on the environment. This observation is confirmed for a large number of other systems systematically analyzed in Ref. 8. Thus, low frequency modes can give especially clear information on specific intermolecular interactions.

Complexes formed by tetramethylpyrazine (TMP) were found to be best suited for our studies.[9] TMP shows the same molecular symmetry as durene. The crystal structure or pure TMP is known.[10,11] Finally, the ability to form complexes being both a π- and an n-electron donor makes TMP mixable with a large number of countermolecules. In this paper the counterpart in the complex is chloranilic acid (CLA) which shows both proton-donor and π-electron-acceptor properties. The mixed material forms a 1:1 hydrogen bonded complex. The crystal structure of the complex was determined recently at $T=100$ K.[12] The lattice consists of infinite chains along the a axis with strong hydrogen bonds (Fig. 1), while the TMP and CLA rings are stacked along the b axis (monoclinic, space group $P2_1/c$, $Z=2$). The irreducible unit of tetramethylpyrazine is half a molecule with two inequivalent methyl groups. In the packing a decisive role is played by hydrogen bond interactions. In addition to the main O–H···N bridges (without proton transfer) unconventional C–H···O and C–H···Cl hydrogen bonds are present which are expected to affect the dynamical behavior of CH_3 groups.

Because, as has been deduced from the doubling of the unit cells,[13] the TMP·CLA crystal undergoes a phase transition at ca. 82 K, we decided to perform detailed structural studies at room temperature and 14 K for samples with both nondeuterated and deuterated OH···N bridges. It seemed to us important to get information about the isotope effect for further investigations on the methyl group rotational potential.

The cell doubling is consistent and required by the number of methyl tunneling bands observed by neutron spectroscopy.[9] Three transitions are found at 29, 21, and 3.3 μeV. The most intense latter one is most likely a superposition of two bands. While the line at 21 μeV is rather insensitive to temperature, the two other transitions follow the normal shift towards the elastic line while broadening. The experiment on a powder sample did not allow a correlation with the position of the methyl groups in the structure.

Besides the fundamental question on the special intermolecular interaction of TMP·CLA dimers which leaves its fingerprint in the CH_3 group dynamics the complexes of CLA can be interesting from the point of view of materials science. It has been pointed out that CLA can be treated as a component of supramolecular synthons in crystal engineering[14] and, belonging to benzoquinones, is interesting from the point of view of the electron transfer processes including biological systems.[15,16] But most interesting seem to be the complexes of CLA with nitrogen bases such as pyridine and diazines,[17] pyrazole and imidazole,[18] and, above all, pyrimidine and pyrazine.[19]

The present work shall extend the previous study[9] towards the reaction of the complex on deuteration of the hydrogen bond and on pressure. Due to the central role of hydrogen bonds for the properties of charge transfer materials we expect characteristic changes from the interplay of lattice contraction, molecular reorientation, and charge redistribution.

To get some additional insight to these questions we decided to perform density functional theory (DFT) calculations of the structure and torsional vibrations for the model system of TMP with two adjacent HF molecules and compare this with the results obtained for TMP and TMP^+.

II. THEORY

The standard description of rotational tunneling and quasielastic scattering is the single particle model (SPM).[1]

SPM is a mean field theory. The environment of the molecule is represented by a rotational potential $V(\varphi)$. Due to the symmetry of the methyl group it is expressed in the form of a Fourier expansion of threefold symmetry up to order J,

$$V(\varphi) = \sum_{j=1}^{J} \frac{V_{3j}}{2}(1 - \cos(3j\varphi - \varphi_{3j})). \quad (1)$$

At low temperatures when the classical rotational jump dynamics is frozen this potential determines the excitations of the hindered quantum rotor by the eigenvalues E_i of the stationary single particle Schrödinger equation[1,2]

$$\left\{ -B\frac{\partial^2}{\partial\varphi^2} + V(\varphi) \right\} \psi_i = E_i \psi_i. \quad (2)$$

Here $B=\hbar^2/2\Theta=0.655$ meV is the rotational constant of the methyl group with the moment of inertia Θ. The tunnel splitting is the difference between the two lowest levels $\hbar\omega_t = E_1 - E_O$. The knowledge of further transitions to higher rotational states, $E_j - E_i$, must be known if the shape of the rotational potential shall be refined.

Pressure changes δp affect intermolecular distances r according to

$$\frac{\delta r}{r} = -\frac{1}{3}\kappa\delta p \quad (3)$$

with the volume compressibility κ as characteristic material parameter. For a Lennard-Jones-type intermolecular interaction potential,

$$V_{\mathrm{LJ}} = ar^n + br^{-6}, \quad (4)$$

the repulsive part with exponents n generally between 9 and 12 becomes relevant with increasing pressure. Therefore a rotational potential increases with increasing pressure to a first approximation as

$$V(\varphi, r) = V(\varphi, r_o)\left(1 - n\frac{\delta r}{r_o}\right). \quad (5)$$

This leads to positive Grüneisen parameters of lattice modes but to negative ones for tunneling modes: the overlap of molecular wave functions diminishes with increasing rotational potential/pressure. The outlined behavior is expected for materials where all intermolecular distances change with pressure affinely and when the interaction parameters are independent of pressure.

High resolution neutron spectroscopy was an especially successful technique to observe the low energy transitions of weakly hindered rotors.[2] The scattering function due to transitions within the tunnel split ground state is very clear.[1,2] We therefore construct the scattering function of the sample under study for $N=4$ inequivalent methyl groups of occurrence probabilities $p(n)$ in TMP and $M=2$ individual protons in the CLA molecule which scatter only elastically. We obtain

$$S(Q,\omega) = \left(\left(\frac{5}{4} + \frac{4}{3}j_o(Qd)\right) + \frac{M}{N}\right)\delta(\omega) + \sum_{n=1}^{N} p(n)\left(\frac{2}{3} - \frac{2}{3}j_o(Qd)\right)\{\delta(\omega+\omega_{tn}) + \delta(\omega-\omega_{tn})\} \quad (6)$$

with the tunnel splittings $\hbar\omega_{\mathrm{tn}}$, momentum transfer Q, and distance d of the protons within one methyl group. For fully resolved tunneling bands the theory yields a ratio between an inelastic band and the total elastic intensity, excluding Bragg scattering, $I_{\mathrm{inel}}(n)/I_{\mathrm{el}} = p(n)(2-2j_o)[5+4j_o+3(M/N)]$, which below shall be compared to the experiment. If a tunnel splitting is not resolved the related inelastic transition is included in the elastic line with an obvious modification of the outlined equation.

III. EXPERIMENT AND CALCULATIONS

A. X-ray diffraction

Single crystal x-ray diffraction data were collected using an automatic x-ray four-circle Xcalibur diffractometer (Oxford Diffraction Company) with charge-coupled device area detectors. Graphite monochromated Mo $K\alpha$ radiation was generated at 50 kV and 25 mA. A single image for 1° rotation around the ω axis was obtained in 30 s. The intensities of the reflections were recorded in 900 frames. At 14 K measurements were performed using an Xcalibur diffractometer with a HeliJet helium cryogenic attachment. The full data collection was performed at 14.0 ± 0.2 and 293.0 ± 0.4 K. The temperature dependence of the lattice parameters and the intensity of selected reflections were measured while changing the temperature of the crystal within the range from 14 to 90 K. Details of data collection and structure refinements are presented in Table I.

The crystal structures of the phases stable at low (14 K) and high (293 K) temperatures were solved using the direct method program SHELXL-97.[20] The same program was used for the successive refinement cycles of the crystal structure.

B. Neutron spectroscopy

Rotational tunneling bands under pressure were measured at the IN10 backscattering spectrometer of the ILL, Grenoble.[21] To observe all tunneling bands found at normal pressure two setups of the instrument had to be used. Using the $CaF_2(111)$ monochromator crystal with an energy offset of 24 μeV, transitions between −36 and −12 μeV were detected, while with the standard Si(111) monochromator all further transitions down to the resolution limit of the instrument of $\delta E_{\mathrm{res}}=0.9$ μeV could be measured. A sample holder containing $10\times30\times2$ mm^3 of polycrystalline material was introduced into a standard He gas pressure cell of the ILL. The small sample volume together with the thick wall of the pressure cell leads to a significant worsening of the signal to noise ratio. The flat sample was oriented under −45° to the neutron beam. Thus the large momentum transfer angles which show the strongest signal according to Eq. (6) are used in reflection geometry. The pressure in the cell was measured

TABLE I. Crystal data and structure refinement for TMP·CLA and deuterated TMP·CLA-d_2 complexes.

	TMP·CLA	TMP·CLA	TMP·CLA-d_2	TMP·CLA-d_2
Empirical formula	C_{14}, H_{14}, Cl_2, N_2, O_4	C_{14}, H_{14}, Cl_2, N_2, O_4	C_{14}, H_{12}, D_2, Cl_2, N_2, O_4	C_{14}, H_{12}, D_2, Cl_2, N_2, O_4
Formula weight	345.17	345.17	347.17	347.17
Temp. (K)	293(2)	14(2)	293(2)	14(2)
Wavelength (Å)	0.710 73	0.710 73	0.710 73	0.710 73
Crystal system	Monoclinic	Monoclinic	Monoclinic	Monoclinic
Space group	$P2_1/c$	$P2_1/n$	$P2_1/c$	$P2_1/n$
Unit cell dimensions				
a (Å)	12.383(3)	13.342(3)	12.4576(18)	13.380(3)
b (Å)	4.712 0(9)	4.693 0(9)	4.7269(7)	4.690 0(9)
c (Å)	13.717(3)	24.622(5)	13.752(2)	24.611(5)
β (°)	105.53(3)	105.40(3)	105.548(14)	105.40(3)
Volume (Å^3)	771.3(3)	1486.3(5)	780.2(2)	1489.0(5)
Z, D_c (mg m^{-3})	2, 1.487	4, 1.543	4, 1.529	4, 1.540
μ (mm^{-1})	0.440	0.456	0.434	0.455
F(000)	356	712	356	712
Crystal size (mm)	$0.32\times0.26\times0.24$	$0.38\times0.26\times0.24$	$0.38\times0.26\times0.24$	$0.34\times0.28\times0.24$
θ range (°)	3.42–29.51	4.01–30.73	4.58–36.31	3.17–29.10
Limiting indices	$-16\leqslant h\leqslant 16$, $-6\leqslant k\leqslant 5$ $-18\leqslant l\leqslant 19$	$-18\leqslant h\leqslant 18$, $-6\leqslant k\leqslant 3$ $-34\leqslant l\leqslant 34$	$-16\leqslant h\leqslant 20$, $-5\leqslant k\leqslant 7$ $-22\leqslant l\leqslant 17$	$-15\leqslant h\leqslant 18$, $-3\leqslant k\leqslant 6$ $-31\leqslant l\leqslant 33$
Reflections collected/unique	8487/1974 R(int)=0.038 5	9604/4120 R(int)=0.056 2	12124/3338 R(int)=0.017 8	9500/3528 R(int)=0.060 9
Completeness to θ=29.51°	91.4%	89%	88.4%	87.8%
Refinement method	Full-matrix least squares on F^2	As previously	As previously	As previously
Data/restraints/ Parameters	1974/0/129	4120/0/256	3338/0/129	3528/0/256
Goodness of fit on F^2	1.057	1.182	0.959	1.125
Final R indices $[I>2\sigma(I)]$	$R1$=0.036 3, $wR2$=0.094 7	$R1$=0.045 4, $wR2$=0.089 2	$R1$=0.030 9, $wR2$=0.066 3	$R1$=0.045 4, $wR2$=0.114 1
R indices (all data)	$R1$=0.043 7, $wR2$=0.101 7	$R1$=0.083 5, $wR2$=0.105 5	$R1$=0.072 0, $wR2$=0.069 6	$R1$=0.062 6, $wR2$=0.124 1
Extinction coefficient	0.094(2)	0.000 0(2)	0.004 8(5)	0.000 6(6)
Largest diff. peak and hole, e Å^{-3}	0.269 and −0.281	0.590 and −0.679	0.311 and −0.204	0.764 and −0.857

by strain gauges which were calibrated after the experiment and corrected for temperature effects. The pressure values given in this text represent corrected values.

Tunneling of the sample with deuterated hydrogen bonds was studied at the BSS backscattering spectrometer of Forschungszentrum Jülich.[22] Two setups of the spectrometer were used. The range $-31\leqslant\Delta E[\mu\text{eV}]\leqslant+3$ is accessible with a SiGe offset monochromator at an energy resolution $\delta E_{\text{res}}=1.56$ μeV. With improved energy resolution $\delta E_{\text{res}}=0.99$ μeV a symmetric spectrum is registered with the Si monochromator for energy transfers $-17\leqslant E[\mu\text{eV}]\leqslant+17$.

Lattice dynamical excitations were measured at the spectrometer SV29 of Forschungszentrum Jülich.[22] A wavelength $\lambda=1.76$ Å was used. The samples had thicknesses of 0.5 mm and were oriented under an angle of −45°.

C. Preparation and infrared spectra

Crystals of the TMP·CLA complex were obtained as previously reported.[12] Deuterated crystals were prepared by a slow evaporation of equimolar solution of TMP and deuterated chloranilic acid in acetone-d_6. The process was performed in Nitrogen Dry Box PLAS LABS. The deuteration degree was estimated based on the IR spectra to be (90±5).

The IR spectra were recorded in fluorolube suspensions on a Fourier transform infrared Bruker IFS 113ν spectrometer.

D. Calculations

DFT calculations [B3LYP/6-311G(d,p) tending towards the optimized structure of the TMP(HF)$_2$ complex and internal frequencies] were performed by using GAUSSIAN program.[7]

IV. RESULTS AND DISCUSSION

A. X-ray diffraction

In the crystalline lattice of TMP·CLA complex chains of alternating donor and acceptor molecules are formed via O–H···N hydrogen bonds, as shown in Fig. 1. The fragments of those chains with atom numbering for room temperature

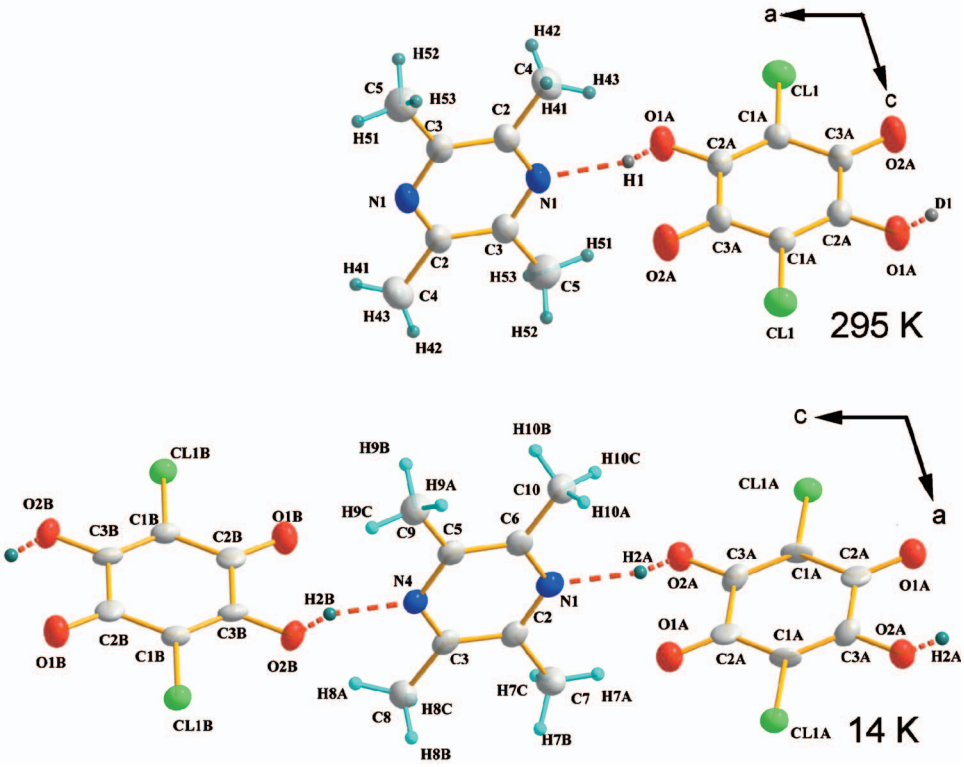

FIG. 2. (Color) Structure and atom numbering of TMP·CLA complex. Top: $T=293$ K, displacement ellipsoids at the 50% probability level. Bottom: $T=14$ K, ellipsoids at the 50% level.

(*A*) and 14 K (*B*) are presented in Fig. 2. As has already been reported,[12] almost perfectly planar core rings of TMP and CLA molecules are oriented to each other at room temperature at the angle equal to 84.4(1)°. All the hydrogen bonds in the chains are at room temperature equivalent. In the cited paper[12] all data related to the geometry of interacting molecules were put together. In the present paper we would like to report the results of structural studies at 14 K and H/D isotope effects for 293 and 14 K. The detailed data with respect to the atomic coordinates with isotropic displacement parameters for H atoms and anisotropic displacement parameters for non-H atoms and all crystallographic data are deposited at the Cambridge Crystallographic Data Center (CCDC No. 627231-627234).

Here we want to discuss the problem of the low temperature phase transition, the features of O–H···N hydrogen bonds, the structural and IR spectroscopic isotope effects, and the environment around the methyl groups for understanding the spectrum of tunneling transitions which is the main task in the present work.

The suggested low temperature phase transition can be investigated by the observation of the intensities of x-ray (422) and (421) reflections. Miller indices are based on the low temperature unit cell. Figure 3 shows the intensities of reflections (422) and (421) versus temperature. The (421) reflection is a superstructure reflection, whose intensity disappears above $T_c=82$ K (±3 K). A temperature point with the zero intensity of (421) is marked at the temperature of phase transition. At the transition a doubling of the unit cells with alternation of hydrogen bond lengths takes place. Half of them becomes somewhat shorter and the second one longer. The quantitative data reflecting this phenomenon along with information on the isotope effect are collected in Table II.

In conclusion one can tell that the decrease of temperature leads not only to the doubling of unit cells and alternation of hydrogen bonds but also to a slight but marked shortening of hydrogen bridges. At temperatures above T_c in the face of equivalency of hydrogen bonds the methyl groups are divided into two sets of equivalent groups, so that we are dealing with two types of methyl groups which differ in the environment. At temperatures below T_c, due to the alternation of hydrogen bonds, an additional differentiation of methyl groups takes place. However, two of them are characterized by rather similar properties ascribed to only slightly different environments.

One should stress here that the core rings of CLA mol-

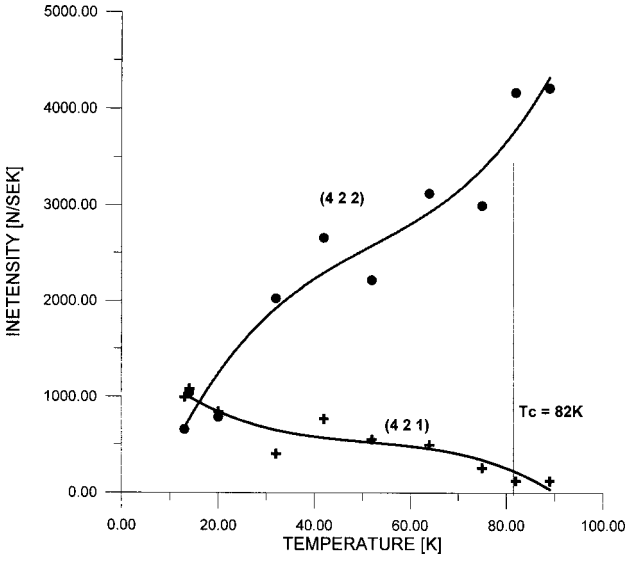

FIG. 3. Plots of intensity of (422) and (421) peaks vs temperature.

TABLE II. Hydrogen bonds for two isotopomers of TMP·CLA at room temperature and 14 K. Symmetry transformation used to generate equivalent atom 3 are $-x+1, -y, -z+1$.

	d(O–H) (Å)	d(H···N) (Å)	d(O···N) (Å)	<OHN (°)
		293 K		
O(1*A*)–H(1)···N(1) 3	0.938(8)	1.824(9)	2.7079(8)	155.9(8)
O(1*A*)–D(1)···N(1) 3	0.879(4)	1.894(5)	2.7295(6)	158.1(1)
		14 K		
O(2*B*)–H(2*B*)···N(4)	0.87(4)	1.84(4)	2.668(2)	158(3)
O(2*A*)–H(2*A*)···N(1) 3	0.85(3)	1.90(3)	2.714(2)	159(3)
O(2*B*)–D(2*B*)···N(4)	0.942(11)	1.783(12)	2.6746(11)	156.8(11)
O(2*A*)–D(2*A*)···N(1) 3	0.904(11)	1.845(12)	2.7172(11)	161.5(11)

ecules attached to the same TMP molecule are below T_c not coplanar as they are above T_c. The dihedral angle of inclination equals to 11.05° for protonated and 10.90° for deuterated species.

As usual in hydrogen bonded systems, one observes the Ubbelohde effect[23] which is characterized by the elongation of bridges on deuteration. This effect is assigned[24,25] to the anharmonicity of the potential for the H/D motion. In the fundamental vibrational levels proton is shifted to the center of the bridge more than deuteron making D bonding weaker than H bonding. In the IR absorption spectrum the stretching absorption band shifts from $\nu(\mathrm{OH})=2750$ to 2060 cm^{-1} after deuteration so that the isotopic ratio $\nu(\mathrm{OH})/\nu(\mathrm{OD})$ equals to 1.33. This value is only a little lower as that expected for harmonic oscillators. However, if one takes into account the structural data it follows that, due to some weakening of hydrogen bonds on deuteration, the charge transfer degree for deuterated bridges should be a little lower than for nondeuterated ones.

B. Rotational tunneling

Figure 4 shows some of the high resolution neutron scattering spectra of the protonated complex measured at various hydrostatic pressures. After fitting the peaks by a sum of Gaussian functions the tunneling energies of Table III are obtained and presented as a function of pressure in Figs. 5 and 6. Table III also contains the fitted tunneling energies of the inner transitions. Due to spurious scattering from the pressure cell close to the elastic line these energies are affected with larger systematic errors and the intensities cannot be reliably extracted. A main observation is that only the band with $\hbar\omega_t$ ($P=1$ bar)$=20.6$ μeV shows a typical exponential shift with pressure, while all other bands stay more or less constant.

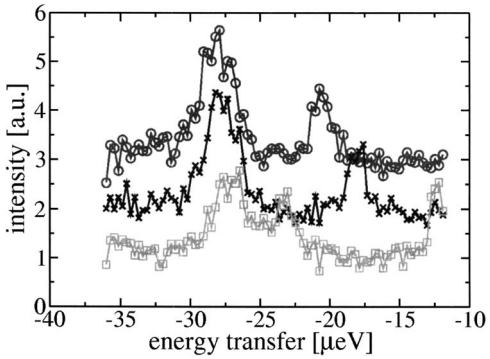

FIG. 4. Selected pressure dependent tunneling spectra of the TMP·CLA complex at 4.5 K under the pressures of 0.001 kbar (○), 0.835 kbar (×), and 3.440 kbar (□); λ=6.27 Å, average momentum transfer $Q=1.6$ $\mathrm{Å}^{-1}$.

It is worth to note that the largest tunnel splitting becomes resolved as a doublet above about 3 kbars. This band was one of the two transitions which showed a too high intensity for the measured low temperature crystal structure. The splitting into two subbands leaves us with a superposition of one spectrum with intensities consistent with the crystal structure and an additional ununderstood line.

At the highest pressure $P=4.2$ kbars the spectrum has lost two tunneling transitions whose intensity is transferred to the surviving two bands. The increased symmetry is indicative that the observed phase transition may have led into the high temperature structure of space group $P2_1/c$ with only two nonequivalent CH_3 groups.

In classical molecular crystals with no pronounced hydrogen bonds the sharper localization of deuterons usually leads to a lattice contraction of the deuterated compound compared to the protonated material with increased potentials and hardened lattice modes. In the present complex the Ubbelohde effect (see above) leads to a very weak expansion

TABLE III. Tunnel splittings of the TMP·CLA complex at $T=4.2$ K.

Pressure (bar)	$\hbar\omega_t$ (μeV)				
	Deuterated H bond				
1	29.2	18.9		3.38	2.02
	Protonated				
1	28.13	20.65		3.31	1.85
352	27.88	19.3			
820				3.2	2.2
835	27.86	18.1			
1615	27.51	16.1		3.1	2.1
2286	27.02	14.66			
2928	27.72	13.39	24.46		
2952				3.05	2.0
3437	27.14	12.20	23.28	3.0	2.0
	Phase transition				
4711		11.80	20.32[a]		1.83

[a]Very weak line.

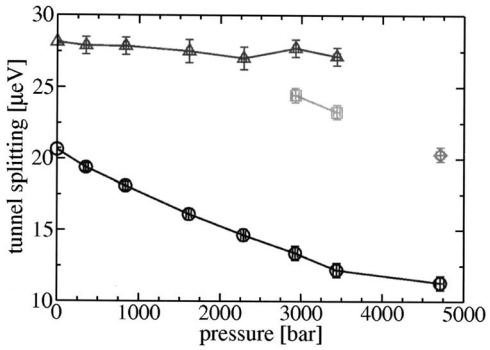

FIG. 5. Evolution of the high energy tunneling splittings with pressure. Sample temperature $T=6$ K. At 3 kbars the degeneracy of the outer line is removed. Phase transition around 4 kbars.

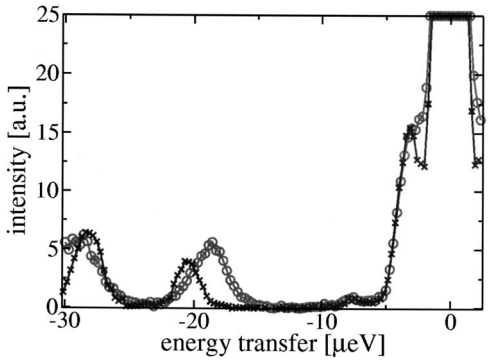

FIG. 7. Comparison of the tunneling spectra of TMP·CLA complex for protonated (×) and deuterated (○) hydrogen bonds. Sample temperature $T=4.5$ K and pressure $P=1$ bar. Instrument BSS, SiGe offset monochromator, FZJ.

of the unit cell in the deuterated compound (Table I). Therefore the response of the lattice dynamics on deuteration is not clear *a priori*. For tunneling hardening means a shift of the tunneling mode towards lower energy. Figures 7 and 8 show a comparison of spectra from the H and the D complex. While the transition at 19 μeV has hardened with deuteration the other modes soften (Table III). The general appearance of the spectrum has changed a little compared to the protonated material. There are still four tunneling bands, but intensities are equal now. This pattern is consistent with the low temperature ($T=14$ K) crystal structure with $Z=4$ dimers in the unit cell with each two related by symmetry and a local twofold axis on the site of the TMP molecule. The different intensities in the protonated compounds remain an unsolved problem.

The temperature dependence of the tunneling spectrum of TMP·CLA-d_2 is shown in Fig. 9. The outmost tunneling peak shifts towards the elastic line and broadens. The peak at 19 μeV shifts first very unusually towards higher energies. Already at $T=23$ K the two lines have almost merged. At the highest temperature of $T=31$ K the contribution of the two high energy tunneling modes to the spectrum looks quasielastic. However, only at this temperature, $T=31$ K, the shift of the inner lines becomes observable. The spectrometer resolution is not good enough, however, to follow this behavior to higher temperature.

The broadening of the transition at 29 μeV with temperature is obtained from numerical fitting. To keep the number of fit parameters small the equal intensity of all tunnel transitions found at the lowest temperature is kept constant for all higher temperatures. Furthermore a common linewidth is attributed to the two outermost tunneling transitions. The such obtained temperature dependence of the linewidth can be fitted by an Arrhenius law with an activation energy of $E_\Gamma^D=8.6$ meV (Fig. 10, squares). For comparison the same broadening is shown for the protonated sample in the same figure (Fig. 10, circles). The activation energy is very similar $E_\Gamma^H=9.4$ meV. The prefactors are similar too with $\Gamma_0 \sim 3$ meV. This value is very consistent with a methyl attempt frequency. According to theory the activation energy should represent the methyl librational energy. A corresponding peak is found in the vibrational density of states at 8.7 meV. This mode shows the expected strong damping of an anharmonic librational mode with temperature.

C. Isotope effect on methyl librations and vibrations

The spectra of TMP·CLA and TMP·CLA-d_2 taken at standard pressure $P=1$ bar in the regime of lattice modes look astonishingly different (Figs. 11 and 12). A weak shift of the band near 8 meV towards lower energy in the D isomer hides the shoulder visible in the protonated sample. The second pronounced band at about 15 meV is lost in the deuterated sample. This could suggest that this band may be due to the proton in the H bond in contrast to the assignment proposed in the previous paper.[9] Thus it becomes difficult to assign just from the experiment librational energies to the

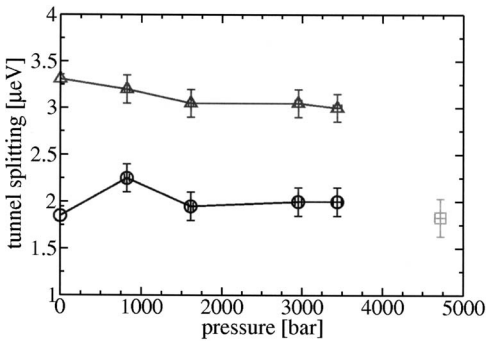

FIG. 6. Evolution of the low energy tunneling splittings with pressure. Sample temperature $T=6$ K.

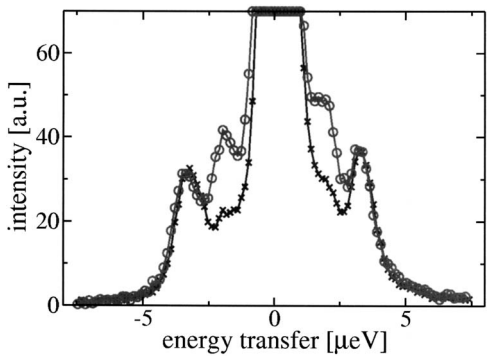

FIG. 8. As Fig. 7 but centered range only with improved energy resolution. Protonated (×) deuterated (○).

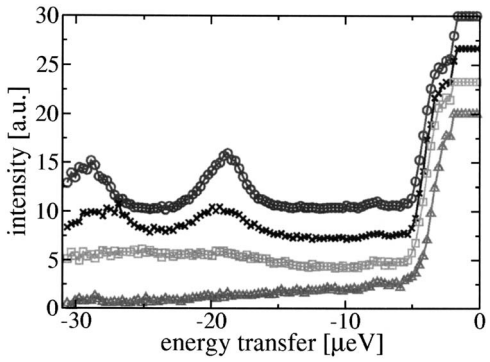

FIG. 9. Temperature evolution of the tunneling spectra of TMP·CLA-d_2 complex. Instrument BSS, offset, FZJ; T=4.5 K (○), 17 K (×), 20 K (□), 31 K (△). The elastic line is cut at intensity=20. The weak peak at 8 μeV is an artifact of the instrument.

stronger hindered methyl group related to the low energy tunneling mode in the D isomer. Since the crystal structure is known a calculation of the phonon dispersion could quantify the amount of mixing of librational modes with other phonons and the corresponding new distribution of intensity. At the moment we have to assume that there is a significant dispersion and combine the almost unchanged weak bands at 13.6 and 17.2 meV into average 15.4 meV librational single particle energies. Such procedure can be justified if accompanied by model calculations. Tunneling and phonon spectra of 2-butine has been reconciled this way.[26] In the present case such an interpretation leads to a rotational potential which is essentially identical to that of the compound with protonated hydrogen bond.[9]

The deuterated compound shows an unusual temperature dependence of the phonon spectrum (Fig. 12). Already its tunnel spectrum was damped much more with temperature than in the protonated material. While just the intensities of bands should change with population of phonon states according to a Bose factor the low librational band overlapping with acoustic phonons looks to soften heavily. The comparison with the same evolution of the protonated compound leads to the conclusion that the 8.4 meV band is purely librational and gets damped with increasing sample temperature while the acoustic phonon branch with its zone boundary energy of ~6 meV gets strongly populated. Due to the close neighborhood of the two lines one observes this intensity change as apparent shift of the whole band. A similar impression is avoided in the protonated compound due to the better separation of the two bands.

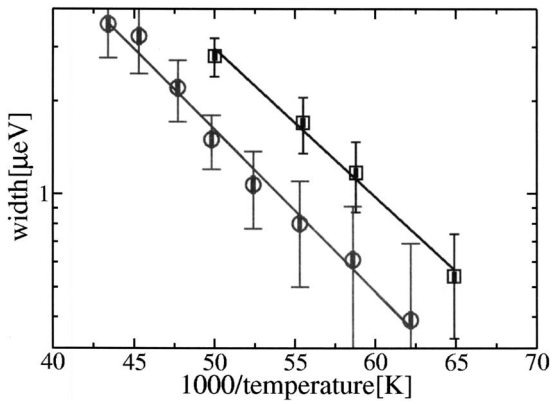

FIG. 10. Temperature evolution of the width of the outmost tunnel transition in TMP·CLA-d_2 (□) compared to the same quantity in TMP·CLA (○). The activation energies are almost equal.

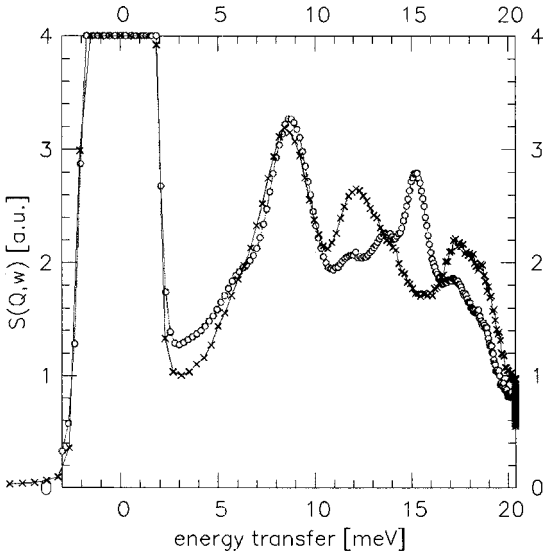

FIG. 11. Spectrum of the TMP·CLA complex in the regime of phonons, T =2.4 K. Protonated (○); deuterated (×). Spectrometer SV29 of FZJ, λ =1.76 Å; average momentum transfer Q=4.0 Å^{-1}.

An actually unsolved question concerns the meaning of the new strong band at 12.1 meV. The weak scattering cross section of deuterium prevents a tempting straightforward assignment as isotopically shifted vibrational band of the hydrogen bond. Alternatively one could identify it as a methyl libration from its strong temperature dependence. The very similar tunneling energies show, however, that the potentials and therewith the librational energies have almost not changed. Model calculations are needed for a final decision.

The final assignment proposed on the basis of this discussion is shown in Table IV.

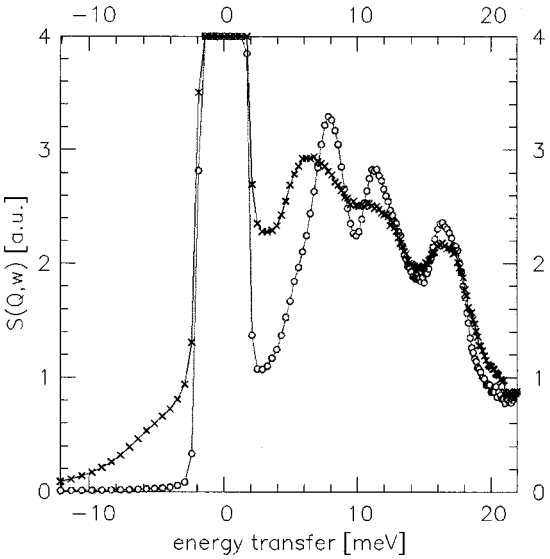

FIG. 12. Spectrum of the TMP·CLA-d_2 complex in the regime of phonons. Sample temperatures: T=2.4 K (○) and T=50 K (×). Spectrometer as in Fig. 11.

TABLE IV. Energies of peaks in the spectra of TMP·CLA and TMP·CLA-d_2. The mode assignment in the regime of phonons is based on consistent interpretation of methyl rotational energies.

TMP·CLA (meV)	TMP·CLA-d_2 (meV)	Intensity ratio H/D	Mode character
5.8	(6.1)		Acoustic mode
8.7	8.4	1	Acoustic mode
	12.1		O–D···N bend?
11.7	12.1	0.1	Lib/phonon
13.6	13.6	1	Lib/phonon
15.2			O–H···N bend?
17.2	17.2	0.3	Lib/phonon
18.3	18.3	0.3	Phonon
24.0	24.2	1	Internal
38		1	Internal

D. Rotational potentials

For protonated TMP·CLA librational and tunneling modes and activation energies had been observed.[9] Rotational potentials which describe the tunnel splittings and activation energies correctly and reproduce the occurrence probabilities of barrier heights are shown in Table V, lines 1–4. They differ very slightly from corresponding values of the previous publication.[9] The librational energies of these potentials do not always coincide with peaks of the vibrational spectra. The presence of dispersion is surely a reason but the argument is unsatisfactory as long as lattice dynamical calculations are not done.

The pressure dependence of rotational potentials can be derived from the shift of tunneling peaks according to Eqs. (5) and (3). We do this for the transition at 20.6 μeV. If we assume that the shape of the potential is unaffected and that only its strength varies with pressure and if we use the value $\kappa=0.021$ kbar^{-1} of solid methane for the unknown compressibility of our material then the evaluation yields $dV_3/dp=1.6$ meV/kbar. This is related with a value $n=5.6$ characterizing the repulsive branch of the intermolecular interaction potential. This value is between $n=7$ expected for electrostatic octopole-octopole interaction and $n=4$ for octopole-monopole interaction. The uncertainty on κ affects this number with some uncertainty.

The pressure dependence of the discussed tunneling transition was assumed to be due to affine changes of the interatomic distances with pressure. We may postulate a same behavior for the environments of the other methyl groups whose tunneling bands almost do not shift with pressure. Then we need a compensation effect which stabilizes the size of the tunnel splitting. This could be charge transfer between the two constituents of the molecular alloy which changes the electrostatic interaction. If the effect is fully attributed to charge transfer δe and assuming multipole-multipole interaction with exponent n we obtain the change of the rotational potential

$$\delta V = \frac{ee}{r^n} - \frac{(e+\delta e)(e+\delta e)}{(r-\delta r)^n} = -2\frac{\delta e}{e} - \frac{n}{3}\kappa\delta p. \tag{7}$$

This expression should be zero. With the parameter values already introduced we obtain $\delta e/e \sim 0.02$/kbar. This means that a 6% reduction of the charge could explain the stability of the tunnel splitting at the pressure of 3.1 kbars. The first principles calculation of neutral and ionized TMP presented in the following section shows that charge transfer reduces the internal contribution to the methyl rotational potential in agreement with the same tendency observed in the TMP·CLA complex.

As long as the pressure dependent structure is not measured the outlined consideration does not represent a unique explanation. It must be kept in mind that distortions of the lattice or the molecule can lead to similar effects.[27]

Finally, we want to estimate the changes of potentials with deuteration of the hydrogen bond, i.e., the OH group of chloranilic acid. If we base this estimate on the shift of tunneling bands we get for the three bands which do not almost shift with pressure weaker rotational potential. The potentials are shown in Table IV. Only the methyl group which shows a normal pressure dependence of tunneling band becomes more strongly hindered. The methyl groups which get in our analysis affected by charge transfer under pressure are weakened already by deuteration of the hydrogen bond. This parallel evolution on two different ways varying the strength of hydrogen bonds, its deuteration and pressure, is a strong argument in favor of the outlined interpretation.

TABLE V. Rotational potentials adjusted for $\hbar\omega_t$ and E_a of TMP·CLA. The fifth line represents the tunnel system with $\hbar\omega_t$ ($P=1$ bar) 20.6 μeV at a pressure $P=3.437$ kbars. Potentials of TMP·CLA-d_2 are only scaled to give the new tunnel splitting.

Sample	P (bar)	Potential V_3 (meV)	Potential V_6 (meV)	$\hbar\omega_t$ (μeV)	E_{01} (meV)	E_a (meV)
TMP·CLA	1	38.0	10.0	1.84	17.0	28.3
	1	36.3	5.0	3.30	14.8	28.0
	1	22.0	4.5	20.6	8.4	15.2
	1	21.0	2.0	28.6	9.8	15.2
	3437	25.4	5.2	12.2	12.2	18.1
TMP·CLA-d_2	1	37.3	9.8	2.02	16.8	27.7
	1	36.1	5.0	3.38	14.7	27.8
	1	22.6	4.6	18.8	11.2	15.7
	1	20.9	2.0	29.2	9.8	15.1

TABLE VI. Neat torsional modes of CH_3 groups in TMP (cm^{-1}).

	Cal.[b]			Expt.[c]	
Mode[a]	TMP	TMP^+	$TMP(HF)_2$	TMP	TMP·CLA
v_2	120	70	116	171	68
v_3	122	71	128	171	74
v_4	140	121	142	190	122
v_5	156	134	159	190	124

[a]Assignment of modes according to Ref. 29.
[b]Calculations for gas phase [DTF/B3LYP 6-31G(d,p)].
[c]From inelastic neutron scattering spectra.

The temperature dependence of the tunneling bands seems to be correlated with its pressure dependence such that the lines with no shift with pressure show a normal shift to lower energies with increasing temperature, while those with significant shift with pressure show a little shift with temperature. A shift of tunneling bands towards higher energies is related to coupling to phonons which modulate the phase of the rotational potential, the so called "shaking" mechanism.[28] Thus a normal pressure behavior is combined with a more unusual coupling mechanism to phonons of a specific symmetry. For the remaining methyl groups the opposite is true: An unusual independence of the band energy on pressure is combined with a standard temperature dependence due to phonon coupling to an amplitude modulation of the rotational potential. This distinction may help in the forthcoming lattice dynamical calculation to identify the respective methyl groups crystallographically.

E. Torsional motion of methyl groups

To get some insight to the role of complexation and the charge transfer effect[29] on the rotational potential we compared the experimental frequencies of torsional modes in the TMP·CLA complex derived from the INS spectra with calculated ones for neat TMP, fully ionized TMP^+, and simple model $TMP\cdot(HF)_2$ complex. Corresponding data are collected in Table VI. The agreement between frequencies found in the TMP·CLA complex and those calculated for TMP cations can suggest an essential role of charge transfer. However, the results obtained for $TMP\cdot(HF)_2$ complex show a minor role of complexation. It seems that three effects contribute to the modification of methyl group rotational potential in TMP molecules reflected in torsional modes. Most general is naturally the intermolecular interaction which leads to the increase of the force constant especially for low frequency modes.[30] The second contribution arises from the binding of the lone electron pairs of nitrogen atoms and creation of modified potential. The third effect should be ascribed to the ionization of molecules and decrease of the charge density in π-electron orbitals.

V. CONCLUSIONS

Lattice dynamics of TMP in the 1:1 complex with chloranilic acid was studied with emphasis on methyl group rotation. Tunneling bands were measured as a function of pressure and deuteration of the hydrogen bonds. The pressure dependence of tunneling systems sorts the methyl groups in two classes, one where pressure has almost no effect on the rotational potential (28, 3.32, and 1.85 μeV) and the other with typical hardening under pressure (20.6 μeV). For the latter the rotational potentials increase with intermolecular distance as $r^{-5.6}$. If one assumes that a similar increase of rotational potentials of the first group is exactly balanced by charge transfer, then a change of relative local charge density $\delta e/e \sim 0.02$ $kbar^{-1}$ is obtained.

At a pressure around 4 kbars the system undergoes a phase transition. The high pressure phase has higher symmetry with only two inequivalent methyl groups/tunnel transitions. The bands evolving from the transitions at 28.6 and at 3.32 μeV at ambient pressure disappear.

In deuterated TMP·CLA-d_2 the relative tunnel intensities become equal and consistent with the crystal structure. Methyl rotational potentials at ambient pressure change with deuteration of the hydrogen bond in the percentage regime. While hardening with deuteration is the generally observed tendency the softening of the three methyl rotational potentials with pressure independent tunneling splittings is unusual. It is a consistent behavior in the frame of the outlined interpretation since deuteration must lead to a similar charge transfer as pressure.

In the present experiment pressure and partial deuteration were found to be parameters which can clarify the role of the various factors affecting rotational potentials of methyl groups reflected in tunnel splittings and frequencies of torsional modes in a charge transfer complex. Further effort, especially computational input, is needed to make such research more generally fruitful.

ACKNOWLEDGMENTS

Support from the Polish Ministry of Science and Informatics (Grant No. 4T09A 05125) is acknowledged. This research project has also been supported by the European Commission under the sixth Framework Programme through the Key Action: Strengthening the European Research Area, Research Infrastructures (Contract No. RII3-CT-2003-505925). The authors thank Dr. S. Mattauch for having called our attention to the new low temperature phase of the system studied.

[1] W. Press, *Single Particle Rotations in Molecular Crystals*, Springer Tracts in Modern Physics, Vol. 81 (Springer, Berlin, 1981).
[2] M. Prager and A. Heidemann, Chem. Rev. (Washington, D.C.) **97**, 2933 (1997).
[3] M. Prager, W. I. F. David, and R. M. Ibberson, J. Chem. Phys. **95**, 2473

(1991).
[4] M. R. Johnson and G. J. Kearley, Annu. Rev. Phys. Chem. **51**, 297 (2000).
[5] M. Plazanet, M. R. Johnson, J. D. Gale *et al.*, Chem. Phys. **261**, 189 (2000).
[6] M. A. Neumann, M. R. Johnson, P. G. Radealli, and H. P. Trommsdorff, J. Chem. Phys. **110**, 516 (1999).
[7] M. J. Frisch, G. W. Trucks, H. B. Schlegel *et al.*, GAUSSIAN 03, Rev. C.02, Gaussian, Inc., Wallingford, CT, 2004.
[8] A. Pawlukojc and L. Sobczyk, Trends Appl. Spectr. **5**, 117 (2004).
[9] M. Prager, A. Pawlukojc, L. Sobczyk, E. Grech, and H. Grimm, J. Phys.: Condens. Matter **17**, 5725 (2005).
[10] A. W. M. Braam, A. Eshuis, and A. Vos, Acta Crystallogr., Sect. B: Struct. Crystallogr. Cryst. Chem. **B37**, 730 (1981).
[11] V. R. Thalladi, A. Gehrke, and R. Boese, New J. Chem. **24**, 463 (2000).
[12] W. Sawka-Dobrowolska, G. Bator, L. Sobczyk, E. Grech, J. Nowicka-Scheibe, and A. Pawlukojc, Struct. Chem. **16**, 287 (2005).
[13] S. Mattauch (unpublished).
[14] Md. B. Zaman, M. Tomura, and Y. Yamashita, Chem. Commun. (Cambridge) **1999**, 999; Org. Lett. **2**, 273 (2000); J. Org. Chem. **66**, 5987 (2001).
[15] *Functions of Quinones in Energy Converting Systems*, edited by B. L. Trimpower (Academic, New York, 1982).
[16] J. P. Clinman and M. David, Annu. Rev. Biochem. **63**, 299 (1994).
[17] H. Ishida and S. Kashino, Acta Crystallogr., Sect. C: Cryst. Struct. Commun. **C55**, 1149 (1999).
[18] H. Ishida and S. Kashino, Acta Crystallogr., Sect. C: Cryst. Struct. Commun. **C57**, 476 (2004).
[19] H. Ishida and S. Kashino, Acta Crystallogr., Sect. C: Cryst. Struct. Commun. **C55**, 1714 (1999).
[20] M. Sheldrick, SHELXS-97, program for solution of crystal structure refinement, University of Götingen, 1997.
[21] http://www.ill.fr/YellowBook/IN10/
[22] http://www.fz-juelich.de/iff/Institute/ins/Broschuere NSE/
[23] A. R. Ubbelohde and K. J. Gallagher, Acta Crystallogr. **8**, 71 (1955).
[24] *The Hydrogen Bond: Recent Developments in Theory and Experiments*, edited by P. Schuster, G. Zundel, and C. Sandorfy (North-Holland, Amsterdam, 1976).
[25] M. Ichikawa, J. Mol. Struct. **552**, 63 (2000).
[26] O. Kirstein, M. Prager, M. R. Johnson, and S. F. Parker, J. Chem. Phys. **117**, 1330 (2002).
[27] S. Clough, ILL Annual Report, 1981, p. 300.
[28] W. Häusler, Physikalisch Technische Bundesanstalt Internal Report No. PTB-PG-3, 1990 (unpublished).
[29] A. Pawlukojć, I. Natkaniec, G. Bator, L. Sobczyk, E. Grech, and J. Nowicka-Scheibe, Spectrochim. Acta, Part A **63**, 766 (2006).
[30] A. Pawlukojć, W. Sawka-Dobrowolska, G. Bator, L. Sobczyk, E. Grech, and J. Nowicka-Scheibe, Chem. Phys. **327**, 311 (2006).